Artificial Nonlinearity Generated from Electromagnetic Coupling Metamolecule

Yongzheng Wen and Ji Zhou[*]

*State Key Laboratory of New Ceramics and Fine Processing, School of Materials Science and Engineering,
Tsinghua University, Beijing 100084, People's Republic of China*
(Received 24 October 2016; published 17 April 2017)

A purely artificial mechanism for optical nonlinearity is proposed based on a metamaterial route. The mechanism is derived from classical electromagnetic interaction in a metamolecule consisting of a cut-wire meta-atom nested within a split-ring meta-atom. Induced by the localized magnetic field in the split-ring meta-atom, the magnetic force drives an anharmonic oscillation of free electrons in the cut-wire meta-atom, generating an intrinsically nonlinear electromagnetic response. An explicit physical process of a second-order nonlinear behavior is adequately described, which is perfectly demonstrated with a series of numerical simulations. Instead of "borrowing" from natural nonlinear materials, this novel mechanism of optical nonlinearity is artificially dominated by the metamolecule geometry and possesses unprecedented design freedom, offering fascinating possibilities to the research and application of nonlinear optics.

Nonlinear optics has been thriving since the first observation of the second harmonic generation (SHG) in 1961 [1], and plays an essential role in many optical devices such as frequency up-converters and mixers, nonlinear spectrometers, and new light sources [2]. Over the past half century, with tons of efforts focused on searching new nonlinear materials [3,4], researchers have endeavored to uncover the physical mechanism behind the optical nonlinearity [5]. As a universal phenomenon, nonlinearity is exhibited by almost all materials interacting with sufficiently strong light [6], and various fundamental mechanisms were proposed, such as distortion of the electron cloud, relative motion of nuclei, reorientation of molecules, electrostriction effect, and thermal effect [7]. Despite the fact that these phenomenological theories extensively advanced the development of new nonlinear materials in the past several decades, they are still inadequate to present a clear physics picture and full description of the origin of the nonlinearity, so up till now it is tremendously difficult to achieve the ambitious goal of exactly predicting, rationally designing, and precisely tailoring a nonlinear material.

Metamaterial, a type of artificial material allowing unprecedented control of light and exhibiting intriguing optical properties not found in nature [8–11], may offer an opportunity of realizing custom-design nonlinear properties. Various approaches were reported to introduce the nonlinearity to metamaterials, for example, engineering meta-atoms with nonlinear insertions, such as varactor diodes [12,13], structuring metamaterials with metal films, whose nonlinearity arises from the surface contribution [14,15], and combining conventional nonlinear materials as host media, such as quantum wells [16,17]. With these methods, rapid progress on optical nonlinearity in metamaterials has been reported, including phase mismatch-free [18], electrical control [19,20], and giant nonlinear

susceptibility [21,22]. However, the optical nonlinear responses in almost all the reported nonlinear metamaterials are actually derived from the above-mentioned external nonlinear materials and devices, and metamaterial structures play roles of enhancement on the natural nonlinearity [23], which cannot fulfil the desire of artificially designing the nonlinearity. Lapine *et al.* made a commendable attempt to realize the structure-based artificial nonlinearity by introducing a mechanical degree of freedom to metamaterial [24], but the delay of its response time may limit its application in high frequency due to the slow mechanical displacement of the meta-atoms.

In this work, a purely artificial mechanism for optical nonlinearity based on a classical electromagnetic (EM) interaction between meta-atoms in a metamolecule is proposed. Without the involvement of any natural nonlinear materials, an iconic second-order nonlinear behavior of the metamolecule is described with an explicit EM coupling mechanism and perfectly verified by a series of numerical simulations. The geometric influences on the nonlinear behavior are also studied to demonstrate the ultrahigh design freedom of the artificial nonlinearity.

Taking a careful look at the classical theory of electromagnetism, we can readily reveal anharmonic motion of the electrons driven by the inherently nonlinear magnetic component of the Lorentz force, which has been neglected for a long time in either nonlinear natural crystals or metamaterials [14,23,25], due to the weak magnetic field in EM wave and slow drift velocity of electrons. The electric field enhancement of the split-ring resonator (SRR) has been noticed and studied in various metamaterials [26,27]; however, its enhancement on the magnetic field is comparably less investigated [28,29]. Based on the theoretical conception of the intrinsic nonlinearity of the magnetic force, a metamaterial comprised of EM coupling

metamolecules was designed as illustrated in Fig. 1. The metamolecule consists of two meta-atoms: a cut-wire meta-atom nested within a SRR meta-atom. With the normal incidence of an x-polarized EM wave, a circulating surface current of the SRR at resonance can induce a magnetic field perpendicular to the metamolecule plane, localized inside the SRR and dramatically enhanced by hundreds of times compared with the incident one [28]. Meanwhile, driven by the electric field of the incident wave, the free electrons in the cut-wire meta-atom move in the x direction with a drift velocity, $\vec{v}$. As the cut wire locates inside the enhanced magnetic field, a strong magnetic force orthogonal to the drift velocity is generated. Therefore, the total force applied to the free electrons in the cut-wire meta-atom is $\vec{F}_{\text{total}} = \vec{F}_E + \vec{F}_B = q\vec{E}(\omega)e^{-i\omega t} + q\vec{v} \times \vec{B}(\omega)e^{-i\omega t} + \text{c.c.}$, where c.c. is the complex conjugate, q is elementary charge, t is time, and $\vec{E}(\omega)$ and $\vec{B}(\omega)$ are vectorial amplitudes of the local electric and magnetic fields at angular frequency ω, respectively.

With the EM coupling, the motion of the free electrons in the cut-wire meta-atom can be described by a modified Drude-Lorentz model as

$$m^* \frac{d^2\vec{r}}{dt^2} + m^*\gamma\frac{d\vec{r}}{dt} + m^*\omega_0^2\vec{r}$$
$$= q\vec{E}(\omega)e^{-i\omega t} + q\vec{v} \times \vec{B}(\omega)e^{-i\omega t} + \text{c.c.,} \quad (1)$$

where $\vec{r}$ is the displacement from the equilibrium position, m^* is the effective electron mass, γ is the electron collision rate, and ω_0 is the angular eigenfrequency, which is 0 for the metal and heavily doped semiconductor used in our case. To demonstrate the artificial nonlinearity from the metamolecule without losing generalities, a widely known and first-observed nonlinear process, SHG, was studied as an example. In that case, the drift velocity of the electron is expressed as $\vec{v} = \tilde{\mu}_e\vec{E}(\omega)e^{-i\omega t}$, where $\tilde{\mu}_e$ is the mobility of the free electrons in the Drude model, and the magnetic force becomes

$$\vec{F}_B = q\tilde{\mu}_e\vec{E}(\omega)e^{-i\omega t} \times \vec{B}(\omega)e^{-i\omega t} + \text{c.c.}$$
$$= q\tilde{\mu}_e\vec{E}(\omega) \times \vec{B}(\omega)e^{-i2\omega t} + \text{c.c.} \quad (2)$$

The exhibited second-order term in the magnetic force oscillates the free electrons in an anharmonic way, supplying a clear and designable mechanism of the artificial nonlinearity. However, in most materials, the magnetic force hardly plays a role due to the weak magnetic component in the EM wave, and it points in the direction of the incident wave vector, which is difficult to generate the second-harmonic wave with forward propagation. In this metamolecule, the dramatic enhancement of the localized magnetic field in the SRR makes the magnetic
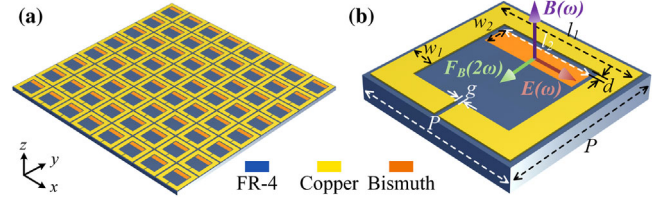

FIG. 1. Schematic of array (a) and unit cell (b) of the metamolecules. The local magnetic and electric fields, and the magnetic force, are marked. In the microwave regime, the geometric constants $l_1 = 3.4$ mm, $w_1 = 0.45$ mm, $g = 0.1$ mm, $l_2 = 2.3$ mm, $w_2 = 0.5$ mm, $d = 0.1$ mm, and $P = 3.6$ mm.

force much more significant. Since the induced magnetic field is along the z axis and the electric field is along the x axis, the magnetic force oscillates the electrons in the cut wire in the y direction, as shown in Fig. 1(b). Hence, it can be expected that the second-harmonic wave radiates along both $+z$ and $-z$ directions in the y polarization. More importantly, this nonlinearity intrinsically originates from the magnetic force rather than the properties of the composites, which fundamentally distinguishes our structure from most reported nonlinear metamaterials [20,23,30].

To physically describe the SHG from the metamolecule and derive the nonlinear polarization, the perturbation method is used to solve Eq. (1), which is evolved into a second-order differential equation by substituting Eq. (2). A displacement with first- and second-harmonic terms is assumed as a general solution, $\vec{r} = \vec{r}_1 + \vec{r}_2 = \vec{r}_1(\omega)e^{-i\omega t} + \vec{r}_2(2\omega)e^{-i2\omega t} + \text{c.c.}$ We separate the first- and second-order terms and rearrange Eq. (1) as

$$m^* \frac{d^2\vec{r}_1(\omega)e^{-i\omega t}}{dt^2} + m^*\gamma\frac{d\vec{r}_1(\omega)e^{-i\omega t}}{dt} = q\vec{E}(\omega)e^{-i\omega t}, \quad (3a)$$

$$m^* \frac{d^2\vec{r}_2(2\omega)e^{-i2\omega t}}{dt^2} + m^*\gamma\frac{d\vec{r}_2(2\omega)e^{-i2\omega t}}{dt}$$
$$= q\tilde{\mu}_e\vec{E}(\omega) \times \vec{B}(\omega)e^{-i2\omega t}. \quad (3b)$$

For clarity, the complex conjugate is eliminated. Equation (3a) presents a similar linear form as the classical Drude model, and its solution is

$$\vec{r}_1(\omega) = -\frac{q}{m^*}G(\omega)\vec{E}(\omega), \quad (4)$$

where

$$G(\omega) = \frac{1}{\omega^2 + i\omega\gamma}. \quad (5)$$

By solving the nonlinear equation Eq. (3b), we can obtain

$$\vec{r}_2(2\omega) = -\frac{q\tilde{\mu}_e}{m^*}G(2\omega)|\vec{B}(\omega)||\vec{E}(\omega)|\hat{a}_y, \qquad (6)$$

where $\hat{a}_y$ is the unit vector along the y axis to indicate orientation of the nonlinear displacement driven by the magnetic force. With Eqs. (4) and (6), the first- and second-order polarizations $[\vec{P}_L(\omega)$ and $\vec{P}_{NL}(2\omega)]$ can be calculated as

$$\vec{P}_L(\omega) = -\varepsilon_0\omega_p^2 G(\omega)\vec{E}(\omega), \qquad (7a)$$

$$\vec{P}_{NL}(2\omega) = -\frac{\varepsilon_0\omega_p^2\mu_{e0}}{1 - i\omega/\gamma}|\vec{B}(\omega)||\vec{E}(\omega)|G(2\omega)\hat{a}_y, \qquad (7b)$$

where ε_0 is the vacuum permittivity, and ω_p and μ_{e0} are the plasma frequency and the dc mobility of the material forming the cut-wire meta-atom, respectively. The mathematical details are described in Sec. I in Supplemental Material [31].

As mentioned above, $\vec{B}(\omega)$ is originally induced by the incident electric field of the EM wave. Hence, according to Ampere's circuital law, $\vec{B}(\omega) \propto \vec{J}(\omega) = \sigma\vec{E}_0(\omega)$, where $\vec{E}_0(\omega)$ is the incident electric field, σ is the conductivity of the SRR, and $\vec{J}(\omega)$ is the surface current density in the SRR. Considering the fact that the strength of the local electric field is basically the same as the incident one, it can be conveniently derived from Eq. (7b) that the nonlinear polarization is in a quadratic relation with the incident electric field, $|\vec{P}_{NL}(2\omega)| \propto |\vec{E}_0(\omega)|^2$, which is a signature phenomenon of the second-order nonlinearity. Meanwhile, the high conductivity of the material composing the SRR would benefit the SHG intensity as well, since it increases the current density and provides stronger magnetic field.

As seen from Eq. (7b), improving the mobility of the cut-wire meta-atom would also strengthen the SHG proportionally. It is because driven by the same electric field, the free electrons would gain higher drift velocity with better mobility, leading to a more significant magnetic force.

To verify our theoretical prediction on the artificial second-order nonlinearity, the metamolecule with the same structure shown in Fig. 1 was modeled and simulated by a commercial finite-element package (comsol Multiphysics), and its geometrical constants were optimized to work in the microwave regime and provide high SHG intensity. Single unit cell was simulated with the periodic boundary (see Sec. II in Supplemental Material [31]). The substrate was 1 mm thick FR-4 with the permittivity of $4.2 + 0.1i$. Guided by the theory, high conductivity of the SRR and high mobility of the cut wire would both benefit the SHG. Accordingly, the SRR is comprised of a 30 μm thick copper layer with the conductivity of 4.5×10^7 S/m [35], and a 100 nm thick bismuth film is modeled as the cut wire with the conductivity (σ_0) of 2.2×10^5 S/m and the mobility (μ_{Bi}) of 0.11 m²/V s [36,37]. All compositions are treated as linear materials in the simulation. To take the localized magnetic field into account, the bismuth film was modeled with an anisotropic conductivity tensor $[\sigma(\omega)]$ derived from a rigorous definition of conductivity including the term of magnetic field (see Sec. III in Supplemental Material [31]) as follows [38,39]:

$$\sigma(\omega) \approx \sigma_0 \begin{bmatrix} \frac{1}{1+(\mu_{Bi}B)^2} & -\frac{\mu_{Bi}B}{1+(\mu_{Bi}B)^2} & 0 \\ \frac{\mu_{Bi}B}{1+(\mu_{Bi}B)^2} & \frac{1}{1+(\mu_{Bi}B)^2} & 0 \\ 0 & 0 & 1 \end{bmatrix}, \qquad (8)$$

where B is the local magnetic field inside the SRR. Despite the utilization of bismuth in this specific implementation, the anisotropic model of conductivity is general and applies to all conductors with the presence of the magnetic field. It should be noted that the bismuth is chosen solely due to its high conductivity and mobility, which enhance the artificial nonlinear response of the metamolecule. As the nonlinearity arises from the metamolecule structure rather than the compositions, other conductors, such as doped silicon, could also be used (see Sec. IV in Supplemental Material [31]).

Under the normal illumination of an x-polarized plane wave from the top, the reflection, transmission, and absorption spectra of the metamolecule were first simulated and plotted in Fig. 2(a). The localized magnetic field reaches its maximum at 10 GHz, which is slightly lower than the resonant frequency of 10.8 GHz. Figure 2(b) shows the surface currents and magnetic field distributions at 10 GHz of the unit cell, and the circulating currents produce the enhanced magnetic field as maximum 79.5 times stronger as the incident one. The existence of the cut wire has no observable influence on the resonance of the SRR, and the induced magnetic field can penetrate through the cut wire due to its thinness.

The time-domain response of the metamolecule was then simulated with a Gaussian pulsed plane wave at 10 GHz casted from the top, and the nonuniformity of the localized magnetic field was taken into account. The peak intensity
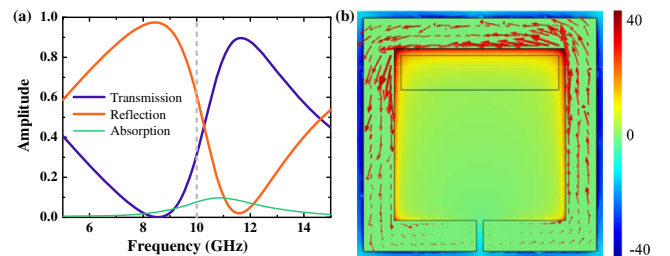

FIG. 2. Transmission, reflection, and absorption spectra of the metamolecule (a) with 10 GHz marked with a grey dashed line; the magnetic field distribution (b) with the scale normalized to the incident magnetic field amplitude and the orientation of the surface currents are marked with red arrows.
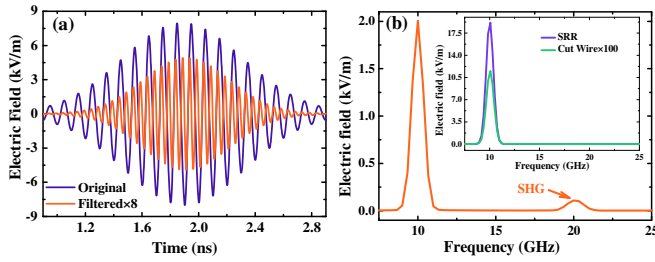
FIG. 3. Original and high-pass filtered time-domain transmission spectra of the nonlinear metamolecule in y polarization (a) and its frequency-domain spectrum (b); the inset is the frequency spectra of two meta-atoms.
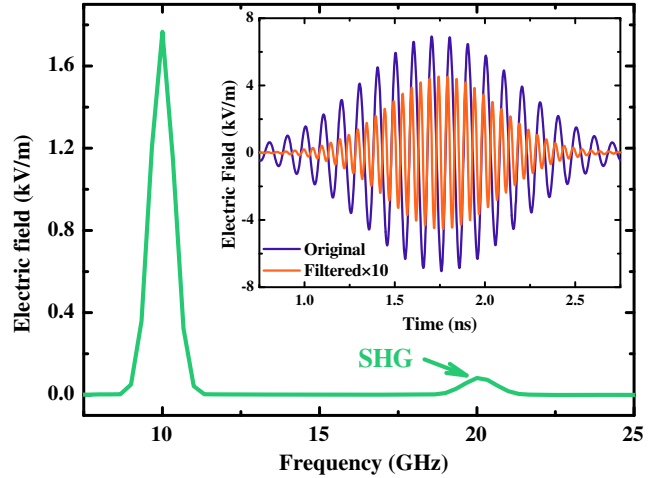

FIG. 4. Reflection frequency spectrum of the metamolecule in y polarization; the inset is its original and high-pass filtered time-domain spectra.

of the incident electric field was 1×10^7 V/m, and the strength of the magnetic force on the free electrons of the cut-wire meta-atom can be theoretically calculated as 29.15% of that of the electric force, which is significant enough to generate a nonlinear response (see Sec. V in Supplemental Material [31]). As revealed in Fig. 3(a), we examined a y-polarized transmission spectrum in time domain, and a 20 GHz wave can be extracted by high-pass filtering with the peak electric field of 613.7 V/m. Compared with the incident fundamental wave, the doubled frequency demonstrates that the proposed metamolecule successfully generates the second-harmonic wave. Because of the weak electric field in the tail bounds of the Gaussian pulse, the pulse width of the SHG signal is narrower than that of the incident wave, resembling the natural nonlinear materials. The frequency spectrum in Fig. 3(b), transformed from the time spectrum by Fourier transformation, exhibits the SHG more obviously. We also observed the x-polarized transmission time and frequency spectra (not shown) but found no SHG. All these simulated results agree perfectly with the theory.

To elucidate the necessity of the EM coupling between the two meta-atoms for the artificial nonlinearity, the metamaterials containing only SRR or cut-wire meta-atoms were simulated with the same incident Gaussian pulsed plane wave at 10 GHz, and the copper of the SRR was modeled with the same anisotropic conductivity tensor and the mobility of 2.25×10^{-3} m^2/V s [40]. Their simulated frequency spectra are revealed in the inset of Fig. 3(b), and there is only a fundamental wave observed and no evident SHG detected. The simulated result of SRR also supports the previously reported hydrodynamic theory that the magnetic contribution to the nonlinear response of the metal SRR can be neglected [25].

As specified in the theory, the proposed metamolecule radiates longitudinally in both directions. Thereby, we examined its y-polarized reflection spectra in frequency and time domains. As shown in Fig. 4, the SHG is also distinct with the peak electric field of 453.1 V/m. Together with the transmitted one, the total conversion efficiency of the metamolecule is calculated as 5.8×10^{-9}, corresponding to an effective second-order nonlinear susceptibility of 1.2×10^3 pm/V (see Sec. VI in Supplemental Material

[31]). This nonlinear susceptibility is not only highly competitive to the reported nonlinear metamaterials based on metal plasmonic resonators [41], but comparable with the traditional nonlinear crystal [6,7].

To confirm that the nonlinearity generated from the metamolecule is capable of artificial manipulation, we studied the relations between the intensity of the transmitted SHG and the two geometric constants of the structure: the distance between two meta-atoms (d), and the width of the cut-wire meta-atom (w_2). Since the nonlinear response is proportional to the magnetic field, which is nonuniformly distributed inside the SRR as depicted in Fig. 2(b), the narrower distance between two meta-atoms locates the cut wire in the region with stronger magnetic field and leads to higher SHG intensity, especially in the range less than 0.1 mm, as plotted in Fig. 5. The inset of Fig. 5 shows the other geometric impact and presents the increase of the cut-wire width enhancing the strength of the SHG in a linear manner. It is easy to understand that the wider resonator means more free electrons can interact with the localized magnetic field, thus leading to a stronger nonlinear response. Inspired by these two examples, it can be conveniently predicted that other geometric constants, which would influence the resonant behavior of the metamolecule, could also have an effective impact on the nonlinear behavior, including the gap (g) and length (l_1) of the SRR, and the lattice constant (P).

All these simulated results adequately verify the proposed mechanism of artificial nonlinearity without involving any sophisticated mesoscopic and quantum mechanisms in materials or low frequency mechanical process. The SRR with cut-wire structure may also play a role in some previously reported nonlinear metamaterials. For example, by designing a split-ring slit combined with a cut-wire slit, Ren *et al.* paved an innovative road of realizing unnaturally giant nonlinear optical activity, in which the origin of the optical nonlinearity
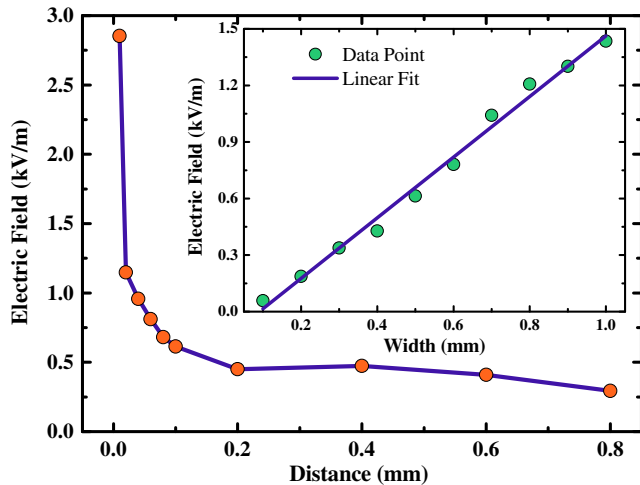
FIG. 5. Relation between the intensity of the transmitted SHG and the distance between two meta-atoms. Inset: the intensity of the SHG with different widths of the cut-wire meta-atom, and the linear fit of the data points.

still resides in gold film instead of the structure [22]. In the design proposed here, the optical nonlinearity essentially arises from a magnetic-force-based EM coupling process, dominated by the metamolecule structure, rather than the electric-field-enhanced natural nonlinearity in most reported work. One convincing proof of the uniqueness of this mechanism is that as described in the physical model above, the second-harmonic wave is actually generated from the cut-wire meta-atom, which is in sharp contrast to the consensus generally held by others that the centrosymmetric cut wire cannot provide SHG [25,42,43].

Instead of borrowing from nature, this artificial mechanism offers metamaterials the ability to generate the optical nonlinearity themselves. More importantly, by simply structuring the inclusion geometry of the metamaterials, the artificial optical nonlinearity can be precisely designed with unprecedented freedom, which would bring unlimited possibilities and myriad novel phenomena to nonlinear optics. Some quick examples may include the flat nonlinear lens and nonlinear holography. Although this proof-of-concept metamolecule is numerically demonstrated in the microwave regime, due to the wide applicability of classical electromagnetism, this theory of artificial nonlinearity can be easily extended to higher frequencies, such as terahertz and infrared (see Sec. VII in Supplemental Material [31]). Meanwhile, the metamolecule is highly feasible in experiment. The microwave and terahertz metamolecules could be conveniently manufactured by microfabrication techniques with standard ultraviolet lithography, and the infrared sample could be processed by nanotechnology with electron-beam lithography. All the metal compositions, such as copper, gold, and bismuth, could be deposited by electron-beam evaporation and magnetron sputtering, and some conductive materials with high mobility may also be involved as the cut-wire meta-atom, such as graphene and InAs.

In conclusion, we theoretically demonstrated a novel mechanism for purely artificial optical nonlinearity generated from a metamolecule consisting of two EM coupled meta-atoms. Interacted with the magnetic field localized in the SRR meta-atom, the free electrons in the cut-wire meta-atom oscillate in anharmonic way under the magnetic force, which generates the nonlinear response. Based on the classical electromagnetism, the physical process of an iconic second-order nonlinearity of the metamolecule is explicitly described and perfectly supported by the numerical simulations. The geometric influences on the nonlinear behavior demonstrate that this innovative mechanism possesses an ultrahigh degree of design freedom. This purely EM mechanism of artificial nonlinearity, without involvement of any photoinduced electronic, thermal, mechanical, or quantum processes in natural materials, supplies a metamaterial-based approach for designing the nonlinear optical materials, which would open a wide range of possibilities and bring fantastic potential to nonlinear optics.

———————

*Corresponding author.
zhouji@tsinghua.edu.cn
 [1] P. Franken, A. E. Hill, C. Peters, and G. Weinreich, Generation of Optical Harmonics, Phys. Rev. Lett. **7**, 118 (1961).
 [2] R. W. Boyd, *Nonlinear Optics* (Academic Press, New York, 2003).
 [3] N. J. Long, Organometallic Compounds for Nonlinear Optics—The Search for En-light-enment!, Angewandte Chemie Int. **34**, 21 (1995).
 [4] S. R. Marder, J. E. Sohn, and G. D. Stucky, Materials for nonlinear optics chemical perspectives, *ACS Symp. Ser.* (American Chemical Society, 1991).
 [5] Z. Kecong and W. Ximin, *Nonlinear Optical Crystal Materials* (Science Press, Beijing 1996).
 [6] Y.-R. Shen, *The Principles of Nonlinear Optics* (John Wiley & Sons, New York, 1984), p. 576.
 [7] G. S. He and S. H. Liu, *Physics of Nonlinear Optics* (World Scientific, Singapore, 1999), Vol. 216.
 [8] M. Khorasaninejad, W. T. Chen, R. C. Devlin, J. Oh, A. Y. Zhu, and F. Capasso, Metalenses at visible wavelengths: Diffraction-limited focusing and subwavelength resolution imaging, Science **352**, 1190 (2016).
 [9] S. Larouche, Y. J. Tsai, T. Tyler, N. M. Jokerst, and D. R. Smith, Infrared metamaterial phase holograms, Nat. Mater. **11**, 450 (2012).
[10] J. Valentine, S. Zhang, T. Zentgraf, E. Ulin-Avila, D. A. Genov, G. Bartal, and X. Zhang, Three-dimensional optical metamaterial with a negative refractive index, Nature (London) **455**, 376 (2008).
[11] X. Ni, Z. J. Wong, M. Mrejen, Y. Wang, and X. Zhang, An ultrathin invisibility skin cloak for visible light, Science **349**, 1310 (2015).

[12] A. Rose, D. Huang, and D. R. Smith, Controlling the Second Harmonic in a Phase-Matched Negative-Index Metamaterial, Phys. Rev. Lett. 107, 063902 (2011).

[13] B. Wang, J. Zhou, T. Koschny, and C. M. Soukoulis, Nonlinear properties of split-ring resonators, Opt. Express 16, 16058 (2008).

[14] M. W. Klein, C. Enkrich, M. Wegener, and S. Linden, Second-harmonic generation from magnetic metamaterials, Science 313, 502 (2006).

[15] S. Linden, F. B. P. Niesler, J. Förstner, Y. Grynko, T. Meier, and M. Wegener, Collective Effects in Second-Harmonic Generation from Split-Ring-Resonator Arrays, Phys. Rev. Lett. 109, 015502 (2012).

[16] K. Fan, H. Y. Hwang, M. Liu, A. C. Strikwerda, A. Sternbach, J. Zhang, X. Zhao, X. Zhang, K. A. Nelson, and R. D. Averitt, Nonlinear Terahertz Metamaterials via Field-Enhanced Carrier Dynamics in GaAs, Phys. Rev. Lett. 110, 217404 (2013).

[17] J. Lee, N. Nookala, J. S. Gomez-Diaz, M. Tymchenko, F. Demmerle, G. Boehm, M.-C. Amann, A. Alù, and M. A. Belkin, Ultrathin second-harmonic metasurfaces with record-high nonlinear optical response, Adv. Opt. Mater. 4, 664 (2016).

[18] H. Suchowski, K. O'Brien, Z. J. Wong, A. Salandrino, X. Yin, and X. Zhang, Phase mismatch-free nonlinear propagation in optical zero-index materials, Science 342, 1223 (2013).

[19] L. Kang, Y. Cui, S. Lan, S. P. Rodrigues, M. L. Brongersma, and W. Cai, Electrifying photonic metamaterials for tunable nonlinear optics, Nat. Commun. 5, 4680 (2014).

[20] W. Cai, A. P. Vasudev, and M. L. Brongersma, Electrically controlled nonlinear generation of light with plasmonics, Science 333, 1720 (2011).

[21] N. Nookala, J. Lee, M. Tymchenko, J. S. Gomez-Diaz, F. Demmerle, G. Boehm, K. Lai, G. Shvets, M.-C. Amann, A. Alu, and M. Belkin, Ultrathin gradient nonlinear metasurface with a giant nonlinear response, Optica 3, 283 (2016).

[22] M. Ren, E. Plum, J. Xu, and N. I. Zheludev, Giant nonlinear optical activity in a plasmonic metamaterial, Nat. Commun. 3, 833 (2012).

[23] M. Lapine, I. V. Shadrivov, and Y. S. Kivshar, Colloquium: Nonlinear metamaterials, Rev. Mod. Phys. 86, 1093 (2014).

[24] M. Lapine, I. V. Shadrivov, D. A. Powell, and Y. S. Kivshar, Magnetoelastic metamaterials, Nat. Mater. 11, 30 (2012).

[25] C. Ciracì, E. Poutrina, M. Scalora, and D. R. Smith, Origin of second-harmonic generation enhancement in optical split-ring resonators, Phys. Rev. B 85, 201403 (2012).

[26] M. Liu, H. Y. Hwang, H. Tao, A. C. Strikwerda, K. Fan, G. R. Keiser, A. J. Sternbach, K. G. West, S. Kittiwatanakul, J. Lu, S. A. Wolf, F. G. Omenetto, X. Zhang, K. A. Nelson, and R. D. Averitt, Terahertz-field-induced insulator-to-metal transition in vanadium dioxide metamaterial, Nature (London) 487, 345 (2012).

[27] M. Choi, S. H. Lee, Y. Kim, S. B. Kang, J. Shin, M. H. Kwak, K. Y. Kang, Y. H. Lee, N. Park, and B. Min, A terahertz metamaterial with unnaturally high refractive index, Nature (London) 470, 369 (2011).

[28] N. Kumar, A. C. Strikwerda, K. Fan, X. Zhang, R. D. Averitt, P. C. M. Planken, and A. J. L. Adam, THz near-field Faraday imaging in hybrid metamaterials, Opt. Express 20, 11277 (2012).

[29] N. Liu and H. Giessen, Coupling effects in optical metamaterials, Angew. Chem., Int. Ed. Engl. 49, 9838 (2010).

[30] H. C. Zhang, Y. Fan, J. Guo, X. Fu, and T. J. Cui, Second-harmonic generation of spoof surface plasmon polaritons using nonlinear plasmonic metamaterials, ACS Photonics 3, 139 (2016).

[31] See Supplemental Material at http://link.aps.org/supplemental/10.1103/PhysRevLett.118.167401 for mathematical details of the polarization equations, the simulation settings, the deviation of the anisotropic conductivity tensor, the simulation with doped silicon as cut-wire meta-atom, the calculation of the ratio of the magnetic force to the electric force, the effective nonlinear susceptibility, and the simulated SHG results in infrared regime, which includes Refs. [32–34].

[32] L. Enke, Z. Bingsheng, and L. Jinsheng, Physics of semiconductor, (Publishing House of Electronics Industry, Beijing, 2003), Vol. 133.

[33] M. Ordal, L. Long, R. Bell, S. Bell, R. Bell, R. Alexander, and C. Ward, Optical properties of the metals al, co, cu, au, fe, pb, ni, pd, pt, ag, ti, and w in the infrared and far infrared, Appl. Opt. 22, 1099 (1983).

[34] N. P. Armitage, R. Tediosi, F. Levy, E. Giannini, L. Forro, and D. vanderMarel, Infrared Conductivity of Elemental Bismuth under Pressure: Evidence for an Avoided Lifshitz-Type Semimetal-Semiconductor Transition, Phys. Rev. Lett. 104, 237401 (2010).

[35] F. Ding, Y. Cui, X. Ge, Y. Jin, and S. He, Ultra-broadband microwave metamaterial absorber, Appl. Phys. Lett. 100, 103506 (2012).

[36] R. Koseva, I. Mönch, J. Schumann, K. F. Arndt, and O. G. Schmidt, Bismuth Hall probes: Preparation, properties and application, Thin Solid Films 518, 4847 (2010).

[37] Y. Hasegawa, Y. Ishikawa, T. Saso, H. Shirai, H. Morita, T. Komine, and H. Nakamura, A method for analysis of carrier density and mobility in polycrystalline bismuth, Physica (Amsterdam) 382B, 140 (2006).

[38] K. Storm, F. Halvardsson, M. Heurlin, D. Lindgren, A. Gustafsson, P. M. Wu, B. Monemar, and L. Samuelson, Spatially resolved Hall effect measurement in a single semiconductor nanowire, Nat. Nanotechnol. 7, 718 (2012).

[39] J. Sun and J. Kosel, Finite-Element Modeling and Analysis of Hall Effect and Extraordinary Magnetoresistance Effect (INTECH Open Access Publisher, Rijeka, Croatia, 2012), Vol. 119.

[40] C. Kittel, Introduction to Solid State (John Wiley & Sons, New York, 1966).

[41] G. Li, S. Chen, N. Pholchai, B. Reineke, P. W. H. Wong, E. Y. B. Pun, K. W. Cheah, T. Zentgraf, and S. Zhang, Continuous control of the nonlinearity phase for harmonic generations, Nat. Mater. 14, 607 (2015).

[42] M. W. Klein, M. Wegener, N. Feth, and S. Linden, Experiments on second-and third-harmonic generation from magnetic metamaterials, Opt. Express 15, 5238 (2007).

[43] Y. Zeng, W. Hoyer, J. Liu, S. W. Koch, and J. V. Moloney, Classical theory for second-harmonic generation from metallic nanoparticles, Phys. Rev. B 79, 235109 (2009).